

Symmetry characterization of eigenstates in opal-based photonic crystals

F. López-Tejiera* and T. Ochiai

Departamento de Física Teórica de la Materia Condensada, Facultad de Ciencias, Universidad Autónoma de Madrid, 28049 Madrid, Spain

K. Sakoda

Research Institute for Electronic Science, Hokkaido University, North 12 West 6, Kita-ku, Sapporo 060-0812, Japan

J. Sánchez-Dehesa

Departamento de Física Teórica de la Materia Condensada, Facultad de Ciencias, Universidad Autónoma de Madrid, 28049 Madrid, Spain

(Received 5 November 2001; published 24 April 2002)

The complete symmetry characterization of eigenstates in bare opal systems is obtained by means of group theory. This symmetry assignment has allowed us to identify several bands that cannot couple with an incident external plane wave. Our prediction is supported by layer-Korringa-Kohn-Rostoker calculations, which are also performed: the coupling coefficients between bulk modes and externally excited field tend to zero when symmetry properties mismatch.

DOI: 10.1103/PhysRevB.65.195110

PACS number(s): 42.70.Qs, 42.70.Gi

I. INTRODUCTION

Periodic dielectric structures (the so-called photonic crystals) are probably one of the most exciting topics in contemporary physics, not only for their scientific relevance but also because of the remarkable applications that have been suggested, especially for systems with gaps in the visible and infrared range. So, since the first proposal in the late 1980s,^{1,2} many efforts have been devoted to the fabrication of materials with an absolute frequency gap in such regions. However, material engineering of three-dimensional (3D) periodic systems at the relevant length scale (hundreds of nanometers to 1 micron) presents nontrivial technological problems in a straightforward manufacture. Several different self-assembly approaches have been proposed³ and one of the most promising strategies is that based on artificial opal systems.^{4,5}

It is clear that one of the most important aspects of sample characterization relies on a proper understanding of optical measurements. The structures within the reflectance or transmittance spectra are currently related with gaps and pseudogaps in the infinite band structure, but the symmetry properties of their eigenfunctions can also produce unexpected patterns: symmetry-inactive modes (i.e., bands that cannot be coupled with incident light due to symmetry reasons) have been reported in some 2D photonic crystals⁶⁻⁸ and some authors have predicted the same phenomenon to take place in 3D materials as well.⁹⁻¹³ Thus, the classification of eigenmodes according to their symmetry properties can provide us valuable information when comparing our calculation with experimental results.

The aim of this work is to present a complete symmetry characterization of eigenstates for the above-mentioned opal structure. In order to reach this goal, the paper is organized as follows: In Sec. II we introduce the solution of Maxwell equations as an eigenvalue problem that can be restricted to a band-structure calculation. Section III describes the sym-

metry properties of electric field according to group theory. In Sec. IV we present the mode assignment for a bare opal system. The existence of uncoupled modes is discussed in Sec. V. Finally, in Sec. VI we summarize our work.

II. MAXWELL EQUATIONS AND PHOTONIC BAND STRUCTURE

As far as the point at stake is the propagation of light in a dielectric material, we shall concern ourselves with the macroscopic Maxwell equations. If we impose our problem to fulfill some requirements,¹⁴ we can decouple the equations in order to finally arrive to an expression entirely in terms of the magnetic field $\mathbf{H}(\mathbf{r})$,

$$\nabla \times \left(\frac{1}{\varepsilon(\mathbf{r})} \nabla \times \mathbf{H}(\mathbf{r}) \right) = \left(\frac{\omega}{c} \right)^2 \mathbf{H}(\mathbf{r}). \quad (1)$$

With the definition of a suitable differential operator

$$\hat{\Theta} \mathbf{H}(\mathbf{r}) \equiv \nabla \times \left(\frac{1}{\varepsilon(\mathbf{r})} \nabla \times \mathbf{H}(\mathbf{r}) \right), \quad (2)$$

Eq. (1) can be explicitly written as an ordinary eigenvalue problem:

$$\hat{\Theta} \mathbf{H}(\mathbf{r}) = \left(\frac{\omega}{c} \right)^2 \mathbf{H}(\mathbf{r}). \quad (3)$$

The somehow arbitrary definition of $\hat{\Theta}$ ensures the operator to be Hermitian, which implies that its eigenfunctions have several properties that are extremely useful in numerical calculations.¹⁴

In the alternate approach, we can eliminate $\mathbf{H}(\mathbf{r})$ to obtain an equivalent formulation for the stationally electric field. This way of considering the problem results in a generalized eigenvalue equation with the dielectric function playing the role of a new Hermitian operator in the right side:

$$\hat{\Xi}_1 \mathbf{E}(\mathbf{r}) \equiv \nabla \times [\nabla \times \mathbf{E}(\mathbf{r})] = \left(\frac{\omega}{c}\right)^2 \varepsilon(\mathbf{r}) \mathbf{E}(\mathbf{r}) \equiv \left(\frac{\omega}{c}\right)^2 \hat{\Xi}_2 \mathbf{E}(\mathbf{r}). \quad (4)$$

It is clear that both choices provide the correct physics, so the preference for Eq. (3) instead of Eq. (4) (or vice versa) in the numerical evaluations will only depend on our personal convenience.

We finally want to remark that Bloch's theorem can be applied to photonic crystals due to the periodicity of the dielectric function $\varepsilon(\mathbf{r})$. Thus, we can restrict the eigenvalue problem to the calculation of the band structure of our system and therefore rewrite Eqs. (3) and (4) as

$$\hat{\Theta} \mathbf{H}_{\mathbf{k}}^n(\mathbf{r}) = \left(\frac{\omega_n(\mathbf{k})}{c}\right)^2 \mathbf{H}_{\mathbf{k}}^n(\mathbf{r}), \quad (5)$$

$$\hat{\Xi}_1 \mathbf{E}_{\mathbf{k}}^n(\mathbf{r}) = \left(\frac{\omega_n(\mathbf{k})}{c}\right)^2 \hat{\Xi}_2 \mathbf{E}_{\mathbf{k}}^n(\mathbf{r}), \quad (6)$$

where ω is the frequency of the eigenstates, \mathbf{k} the Bloch wave vector within the first Brillouin zone, and n a discrete index for increasing eigenfrequencies.

III. EIGENMODE CHARACTERIZATION

A. Eigenfunctions and symmetry operators

Bloch's theorem states that the electric field within a photonic crystal can be written as

$$\mathbf{E}_{\mathbf{k}}^n(\mathbf{r}) = e^{i\mathbf{k}\cdot\mathbf{r}} \mathbf{u}_{\mathbf{k}}(\mathbf{r}), \quad (7)$$

in which \mathbf{k} is the Bloch wave vector inside the first Brillouin zone and $\mathbf{u}_{\mathbf{k}}(\mathbf{r})$ a periodic vector function of the lattice structure. It follows from the above-mentioned periodicity that

$$\mathbf{E}_{\mathbf{k}}^n = e^{i\mathbf{k}\cdot\mathbf{r}} \sum_{\mathbf{q}} \mathbf{f}_{\mathbf{q}} e^{i\mathbf{q}\cdot\mathbf{r}}, \quad (8)$$

where \mathbf{q} is a reciprocal-lattice vector of the structure.

Let \hat{A} be a symmetry operator of the lattice. The way in which a general symmetry transformation \hat{A} operates over a vector field $\mathbf{f}(\mathbf{r})$ is

$$\hat{A}\mathbf{f}(\mathbf{r}) = A\mathbf{f}(A^{-1}\mathbf{r}). \quad (9)$$

Hence

$$\hat{A}\mathbf{E}_{\mathbf{k}}^n = A\mathbf{e}^{i\mathbf{k}\cdot A^{-1}\mathbf{r}} \sum_{\mathbf{q}} \mathbf{f}_{\mathbf{q}} e^{i\mathbf{q}\cdot A^{-1}\mathbf{r}}. \quad (10)$$

Taking the orthogonality of symmetry matrices into account,

$$\hat{A}\mathbf{E}_{\mathbf{k}}^n = A\mathbf{e}^{iA\mathbf{k}\cdot\mathbf{r}} \sum_{\mathbf{q}} \mathbf{f}_{\mathbf{q}} e^{iA\mathbf{q}\cdot\mathbf{r}}. \quad (11)$$

For a wave vector \mathbf{k} , the \mathbf{k} -vector point group $G_{\mathbf{k}}$ is defined as the set of symmetry operations which satisfy

$$A\mathbf{k} = \mathbf{k} + \mathbf{q}' \quad (12)$$

with \mathbf{q}' in the reciprocal lattice. Thus, \hat{A} being part of $G_{\mathbf{k}}$,

$$\hat{A}\mathbf{E}_{\mathbf{k}}^n = \mathbf{e}^{i(\mathbf{k}+\mathbf{q}')\cdot\mathbf{r}} \sum_{\mathbf{q}} A\mathbf{f}_{\mathbf{q}} e^{iA\mathbf{q}\cdot\mathbf{r}}. \quad (13)$$

Given that the extra phase can always be included in the infinite summatory, we conclude that the symmetry transformation of $\mathbf{E}_{\mathbf{k}}^n(\mathbf{r})$ generates another Bloch function with the same wave vector:

$$\hat{A}\mathbf{E}_{\mathbf{k}}^n = \mathbf{e}^{i\mathbf{k}\cdot\mathbf{r}} \mathbf{v}_{\mathbf{k}}(\mathbf{r}). \quad (14)$$

Let us now consider the action of a symmetry operator \hat{A} on both sides of Eq. (6):

$$(\hat{A}\hat{\Xi}_1)\mathbf{E}_{\mathbf{k}}^n(\mathbf{r}) = \left(\frac{\omega_n(\mathbf{k})}{c}\right)^2 (\hat{A}\hat{\Xi}_2)\mathbf{E}_{\mathbf{k}}^n(\mathbf{r}). \quad (15)$$

For any symmetry operator that leaves $\varepsilon(\mathbf{r})$ invariant within the unit cell, it can be easily proved that it commutes with $\hat{\Xi}_1$ and $\hat{\Xi}_2$. Therefore

$$\hat{\Xi}_1[\hat{A}\mathbf{E}_{\mathbf{k}}^n(\mathbf{r})] = \left(\frac{\omega_n(\mathbf{k})}{c}\right)^2 \hat{\Xi}_2[\hat{A}\mathbf{E}_{\mathbf{k}}^n(\mathbf{r})], \quad (16)$$

which implies both $\mathbf{E}_{\mathbf{k}}^n(\mathbf{r})$ and $\hat{A}\mathbf{E}_{\mathbf{k}}^n(\mathbf{r})$ are eigenfunctions with the same eigenfrequency.

On the assumption that $G_{\mathbf{k}} = \{\hat{A}_i\}$ is the point group of some wave vector \mathbf{k} , it follows from Eqs. (14) and (16) that $\mathbf{E}_{\mathbf{k}}^n(\mathbf{r})$ must verify

$$\hat{A}_i \mathbf{E}_{\mathbf{k},g}^n(\mathbf{r}) = \sum_{g'} \alpha_{g,g'}^i \mathbf{E}_{\mathbf{k},g'}^n(\mathbf{r}), \quad (17)$$

where g is the eigenmode degeneracy. We shall henceforth concern ourselves with the meaning of that set of scalar coefficients $\{\alpha_{g,g'}^i\}$.

B. Theory of representations

Within the framework of the usual group theory,¹⁵ it can be straightforwardly proved that the scalar coefficient matrices $\tilde{\alpha}^i$ in Eq. (17) form a representation of (i.e., are homomorphic with) the $G_{\mathbf{k}}$ group. On the other hand, in the case where the degeneracy is said to be normal (i.e., when it is not possible to remove such a degeneracy by changing a parameter which does not alter the stated symmetry of the problem), it may be seen that the set $\{\mathbf{E}_{\mathbf{k},g}^n(\mathbf{r})\}$ spans an irreducible invariant space under the $G_{\mathbf{k}}$ group of symmetry operators. Thus, the $\{\tilde{\alpha}^i\}$ set of matrices constitutes an irreducible representation R of the $G_{\mathbf{k}}$ point group, and the R label can be therefore assigned to the n th eigenmode at the \mathbf{k} point.

If \hat{A}_i belongs to a class C , then

$$\sum_g \alpha_{g,g}^i = \chi_C^R, \quad (18)$$

with χ_C^R the character of class C in some irreducible representation R . Given that each R has its own characters, we can use them to distinguish the irreducible representations in or-

TABLE I. The symmetry point groups at the corner of the irreducible part of the Brillouin zone in the fcc lattice according to Schoenflies notation. Notice that the components of representative vectors are in units of $2\pi/a$.

Label	Representative \mathbf{k} vector	Symmetry point group
Γ	(0, 0, 0)	O_h
X	(1, 0, 0)	D_{4h}
L	(1/2, 1/2, 1/2)	D_{3d}
U	(1, 1/4, 1/4)	C_{2v}
W	(1, 1/2, 0)	D_{2d}
K	(3/4, 3/4, 0)	C_{2v}

der to classify the different eigenmodes.¹⁶ Further details about character evaluation can be found in Appendix A.

IV. SYMMETRY CHARACTERIZATION IN BARE OPAL SYSTEMS

Synthetic bare opals are constituted by SiO_2 spheres that organize themselves to form a face-centered-cubic (fcc) lattice. As far as this process has been extensively described in previous works,⁴ we just mention that the opaline sample growth method is based on natural sedimentation of silica nanospheres along the (111) direction of the fcc lattice. Although the refractive index contrast between SiO_2 and air does not allow bare opals to exhibit complete gaps, they can be used as templates to obtain the so-called inverted structures,¹⁷⁻²¹ which are one of the most promising strategies between the different self-assembly approaches to photonic crystal fabrication. Thus, no one can deny that bare opals still constitute a topic of present interest.

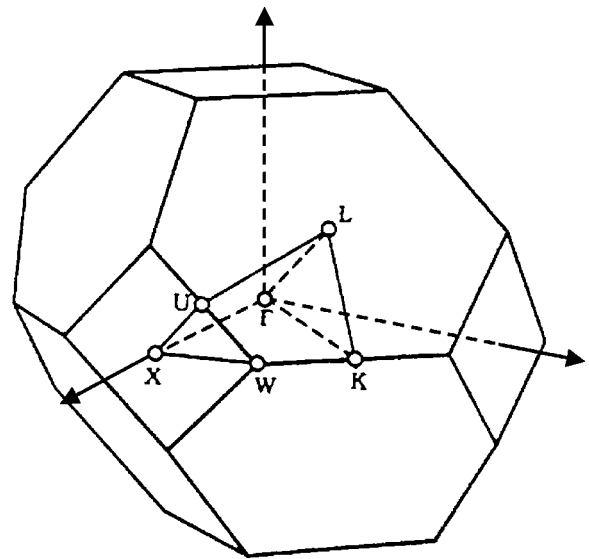


FIG. 1. The first Brillouin zone of the fcc lattice. The lines between white circles define the boundaries of the irreducible part of the zone.

In order to work out the classification of eigenstates described in the previous section, we shall first concern ourselves with the intrinsic properties of the face-centered-cubic lattice, as far as the symmetry point group, which determines the set of allowed irreducible representations for any wave vector \mathbf{k} , is irrespective of the particular realization of our system. Table I lists the symmetry point groups at the corners of the irreducible part of the first Brillouin zone (see Fig. 1) according to Schoenflies notation. Given that the R representation can be assigned to the n th mode at one of those par-

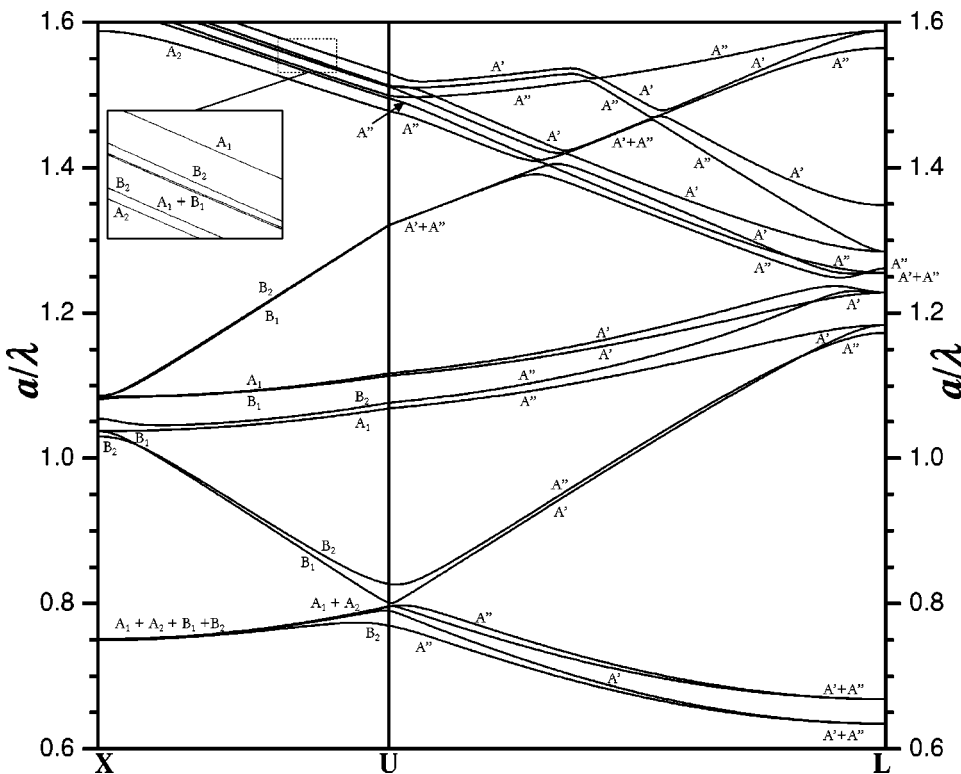


FIG. 2. Photonic band structure along the XU and UL directions for a bare opal system. Labels refer to irreducible representations of C_{2v} and C_{1h} , respectively. An inset figure is included for the sake of clarity. A sum symbol is employed where two or more nondegenerated bands are too close to be distinguished by the naked eye.

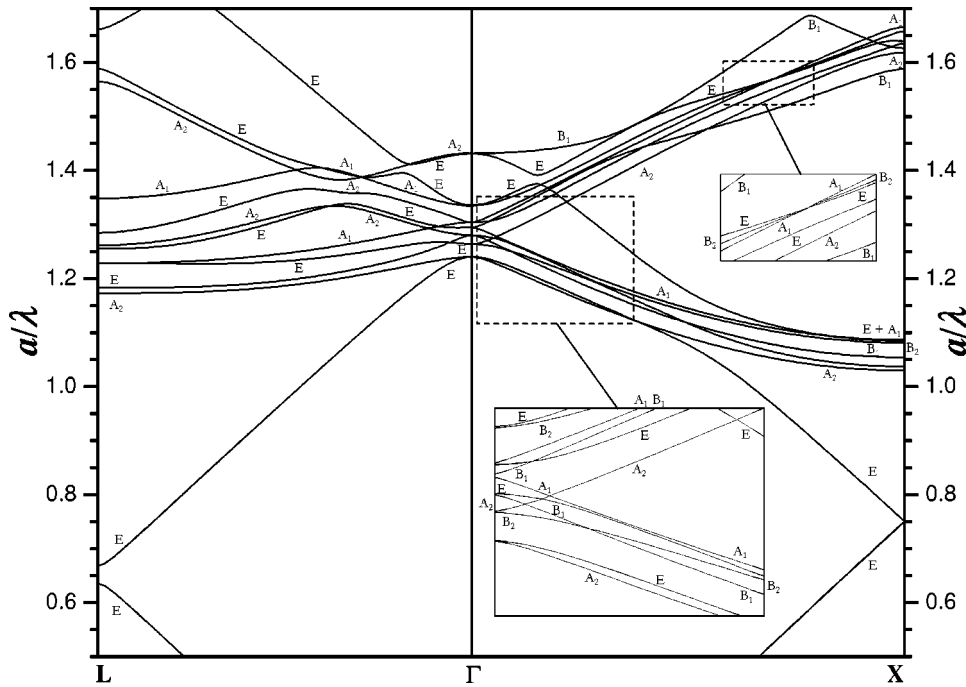


FIG. 3. Photonic band structure along the $L\bar{\Gamma}$ and $\bar{\Gamma}X$ directions for a bare opal system. Labels refer to irreducible representations of C_{3v} and C_{4v} , respectively. Some inset figures are included for the sake of clarity. A sum symbol is employed where two or more nondegenerated bands are too close to be distinguished by the naked eye.

ticular points, we can then easily derive all its compatibility relations (see Appendix B) with the corresponding modes at adjacent wave vectors by following the loss of symmetry as we go from one point group to another which is a subgroup of the first.

In Figs. 2–4 we present the photonic band structure of a face-centered-cubic lattice of spheres. Results are plotted in terms of reduced frequency a/λ where a and λ denote the lattice parameter and the vacuum wavelength, respectively. The dielectric constants of the sphere and the background were assumed to be 2.104 (silica) and 1.0 (air). The ratio of

the lattice parameter and the sphere radius was chosen to verify a close-packing condition. This band calculation was carried out by means of an iterative implementation²² of the plane-wave expansion of Eq. (3). Of course, the photonic band structure of a bare opal system has been previously calculated,²³ so the main outcome of our present work is obviously the mode assignment for the electric field. The labels within the figures have been determined by the numerical evaluation of only several eigenmodes, as far as the above-mentioned compatibility relations allowed us to easily connect the irreducible representations for adjacent wave

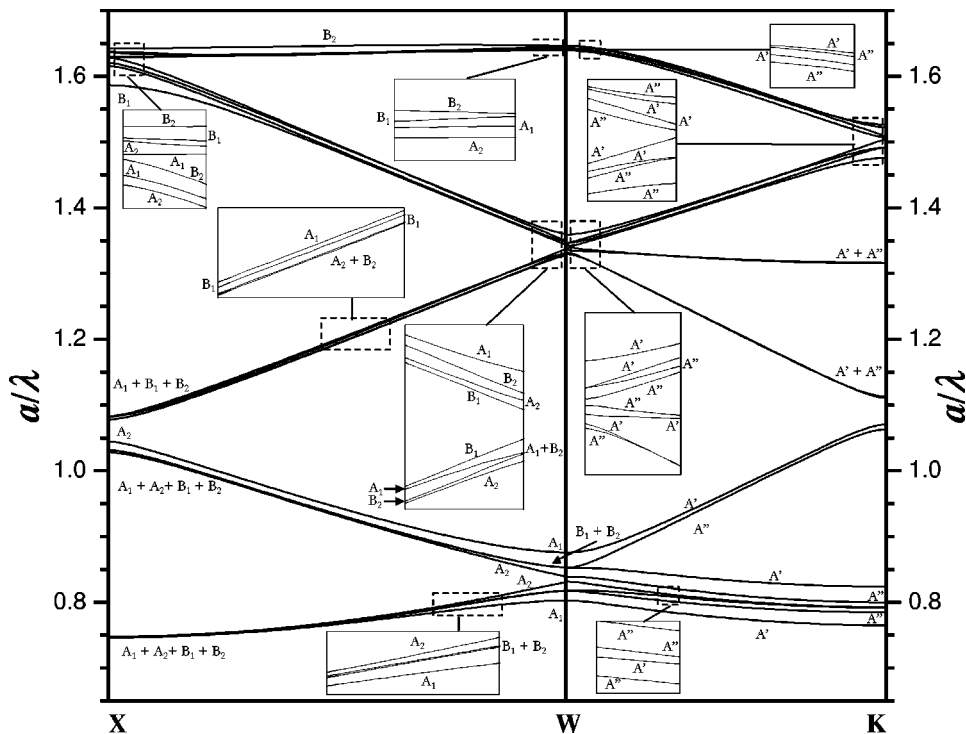


FIG. 4. Photonic band structure along the XW and WK directions for a bare opal system. Labels refer to irreducible representations of C_{2v} and C_{1h} , respectively. Some inset figures are included for the sake of clarity. A sum symbol is employed where two or more nondegenerated bands are too close to be distinguished by the naked eye.

TABLE II. The irreducible representations corresponding to eigenvalues first to twentieth at the corners of the irreducible part of the first Brillouin zone in a bare opal system.

$\Gamma[O_h]$	$X[D_{4h}]$	$L[D_{3d}]$	$U[C_{2v}]$	$W[D_{2d}]$	$K[C_{2v}]$
T_{1u}	E_u	E_g	B_2	A_1	B_2
T_{1g}	E_g	E_u	B_1	E	B_1
E_u	A_{2g}	A_{1u}	A_1	B_1	A_1
T_{2u}	E_g	E_u	A_2	A_2	A_2
E_g	B_{1g}	E_g	B_1	E	B_1
T_{1u}	B_{1u}	A_{1g}	B_2	B_2	B_2
T_{2g}	E_u	E_g	A_2	A_2	A_2
T_{2u}	A_{2u}	A_{2g}	B_2	B_2	B_2
	B_{2u}	E_u	A_1	E	A_1
	A_{1u}	A_{2u}	B_1	B_1	B_1
	B_{1g}	A_{2g}	B_1	A_1	B_1
	E_u	E_g	B_2	B_1	B_2
	E_g	E_u	A_2	A_1	A_2
	B_{2g}		A_2	E	A_2
			B_2		B_2
			B_1		B_1
			A_1		A_1
			B_2		B_2
			A_1		A_1
			B_1		B_1

vectors. For the sake of completeness, we also list in Table II the symmetry characterization of eigenmodes at Γ , X , L , U , W , and K points for increasing values of the eigenfrequency.

V. UNCOUPLED BANDS

A. Symmetry assignment and uncoupled modes

As mentioned in Sec. I, light attenuation produced by uncoupled bands (i.e., bands with eigenmodes that cannot be excited by the incident light because of symmetry reasons) has been reported in some 2D photonic crystals. Moreover, some authors have predicted a similar phenomenon to also take place in 3D materials,^{9–13} but as far as we know, there is no experimental evidence of this mechanism operating in an opaline structure. The exposition of how these uncoupled modes can be identified as a simple consequence of the symmetry assignment will be the aim of the present section.

In order to reach this goal, let us focus our interest on what happens when light incidence is normal to the $\{111\}$ set of planes in the opal. This is the direction along which the structure naturally grows and from which experimental data are usually obtained. If we consider the z axis in the normal direction to the sample surface, the incident plane waves can be expressed in terms of the following vector basis:

$$\{\mathbf{v}_1 = (1,0,0)e^{ikz}; \quad \mathbf{v}_2 = (0,1,0)e^{ikz}\}, \quad (19)$$

where k is the wave number of the plane waves in free space. On the other hand, it is clear that vectors in Eq. (19) also form a basis set of some reducible or irreducible representa-

TABLE III. The representations of incident plane waves (PW) and the subsequent uncoupled bands along some relevant high-symmetry directions in the Brillouin zone of the fcc lattice. Point symmetry groups are described (in brackets) according to Schoenflies notation.

Incidence direction	PW representation	Uncoupled bands
$\Gamma L[C_{3v}]$	E	A_1, A_2
$\Gamma X[C_{4v}]$	E	A_1, A_2, B_1, B_2
$\Gamma K[C_{2v}]$	$B_1 \oplus B_2$	A_1, A_2

tion of the C_{3v} point group. In order to determine that representation, we have to apply the symmetry operations of C_{3v} over the vector basis:

$$\hat{C}_{3z}\mathbf{v}_1 = -\frac{1}{2}\mathbf{v}_1 + \frac{\sqrt{3}}{2}\mathbf{v}_2,$$

$$\hat{C}_{3z}\mathbf{v}_2 = -\frac{\sqrt{3}}{2}\mathbf{v}_1 - \frac{1}{2}\mathbf{v}_2, \quad (20)$$

$$\hat{\sigma}_v\mathbf{v}_1 = -\mathbf{v}_1,$$

$$\hat{\sigma}_v\mathbf{v}_2 = \mathbf{v}_2. \quad (21)$$

From Eqs. (20) and (21) we can obtain the trace (character) of the transformation matrices:

$$\chi(C_{3z}) = -1; \quad \chi(\sigma_v) = 0. \quad (22)$$

If we compare these results with the properties of the C_{3v} point group, we find that these are the characters of the E representation. But the boundary condition of tangential components of the electromagnetic field being continuous at the interface imposes the representation (i.e., the symmetry properties) both inside and outside the system to be the same. Consequently, only E -labeled states will contribute to light transport along the (111) direction of the structure. This kind of restriction in available bands is present in several directions of the lattice, but we are mainly interested in those which include the Γ point, i.e., those in which some observable consequences are expected.

In Table III we summarize the information about uncoupled modes along the relevant directions of a face-centered-cubic structure provided by symmetry considerations. Let there be a frequency range where only uncoupled modes exist. Despite its nonzero density of states, we would expect a total reflection (zero transmission) in such a range as a consequence of photonic states not being coupled with the incidence plane wave.

Unfortunately, this is not the case for bare opal systems: as shown in Figs. 2–4, uncoupled modes always coexist with available ones, and consequently transmittance measurements cannot confirm the predictions of group theory. Therefore, an alternative test will be required.

B. Estimation of the coupling by means of the layer-Korringa-Kohn-Rostoker (KKR) method

It is well known that the photonic band structure of a regular array of nonoverlapping spheres in a host medium can be very accurately calculated within the framework of the layer-KKR method.^{9,24–28} Moreover, we can also obtain the transmission and reflection coefficients through a finite slab of such material combining the scattering matrices of its different layers. On the assumption that slab thickness is very large, the electromagnetic field in the middle of that slab can be regarded as a superposition of the true bulk eigenstates. Thus, a kind of overlapping integral of this field and the actual eigenstates of the infinite system would provide an estimation of the coupling between the structure and the incident light.

Let the z axis be in the normal direction to the slab surface. Hence, the electric field between two consecutive sphere layers can be expressed in terms of its Fourier components as

$$\mathbf{E}_{\text{void}}(\mathbf{r}) = \sum_{\mathbf{q}} \mathbf{u}_{\mathbf{q}}^+ e^{i\mathbf{K}_{\mathbf{q}}^+ \cdot \mathbf{r}} + \mathbf{u}_{\mathbf{q}}^- e^{i\mathbf{K}_{\mathbf{q}}^- \cdot \mathbf{r}}, \quad (23)$$

$$\mathbf{K}_{\mathbf{q}}^{\pm} = \mathbf{k}_{\parallel} + \mathbf{q} \pm \hat{z} \sqrt{\frac{\omega^2}{c^2} - (\mathbf{k}_{\parallel} + \mathbf{q})^2}. \quad (24)$$

Here, \mathbf{q} denotes the 2D reciprocal-lattice vector associated to the surface periodicity, and $\mathbf{k}_{\parallel} \equiv (k_x, k_y)$ the wave vector within the surface Brillouin zone. Given that d is the separation between consecutive layers, these Fourier components also verify

$$Q \begin{pmatrix} \mathbf{u}_{\mathbf{q}}^+ \\ \mathbf{u}_{\mathbf{q}}^- \end{pmatrix} = e^{ik_z d} \begin{pmatrix} \mathbf{u}_{\mathbf{q}}^+ \\ \mathbf{u}_{\mathbf{q}}^- \end{pmatrix}, \quad (25)$$

where Q is an appropriately constructed transfer matrix which relates the electric field in the void between the $(N-1)$ th and N th layers to that between the N th and $(N+1)$ th ones. Since Q is not Hermitian, its left eigenstate

$$u_L = \begin{pmatrix} \mathbf{u}_{\mathbf{q}}^+ \\ \mathbf{u}_{\mathbf{q}}^- \end{pmatrix} \quad (26)$$

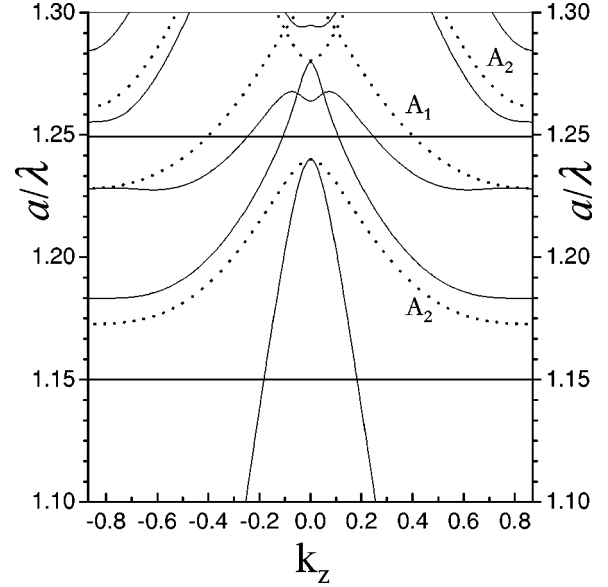


FIG. 5. Detail of the photonic band structure normal to the $\{111\}$ set of planes of a bare opal system. Notice that the maximum value of $|k_z|$ is $\sqrt{3}/2$ in units of $2\pi/a$. The thin horizontal lines define the frequencies at which the branching ratios are obtained. We have to mention that our calculation points out a very small splitting of about 0.014% for E bands which cannot be appreciated in the figure.

is generally different from the complex conjugate of the right one, but we assume that both are normalized to meet the orthogonality condition

$$(u_L^n)^\dagger u_R^{n'} = \delta'_{nn'}. \quad (27)$$

We can then define the coupling coefficient c_n as

$$c_n = (u_L^n)^\dagger u_{\text{bulk}}, \quad (28)$$

with u_{bulk} a column vector which contains the Fourier coefficients of the electric field excited by the incident light in the bulk part of the system.²⁹ Notice that Eq. (28) involves a selection rule on the spatial symmetry of the electric field. Since the transfer matrix Q commutes with the symmetry operations of the point group relevant to the incidence sur-

TABLE IV. The compatibility relations of irreducible representations at the Γ point in the fcc lattice.

$\Gamma[O_h]$	$\overline{\Gamma X}[C_{4v}]$	$\overline{\Gamma U}[C_{1h}]$	$\overline{\Gamma L}[C_{3v}]$	$\overline{\Gamma K}[C_{2v}]$	$\overline{\Gamma W}[C_{1h}]$
A_{1g}	A_1	A'	A_1	A_1	A'
A_{2g}	B_1	A''	A_2	B_2	A'
E_g	$A_1 \oplus B_1$	$A' \oplus A''$	E	$A_1 \oplus B_2$	$2A'$
T_{1g}	$E \oplus A_2$	$A' \oplus 2A''$	$E \oplus A_2$	$A_2 \oplus B_1 \oplus B_2$	$A' \oplus 2A''$
T_{2g}	$E \oplus B_2$	$2A' \oplus A''$	$E \oplus A_1$	$A_1 \oplus A_2 \oplus B_1$	$A' \oplus 2A''$
A_{1u}	A_2	A''	A_2	A_2	A''
A_{2u}	B_2	A'	A_1	B_1	A''
E_u	$A_2 \oplus B_2$	$A' \oplus A''$	E	$A_2 \oplus B_1$	$2A''$
T_{1u}	$E \oplus A_1$	$2A' \oplus A''$	$E \oplus A_1$	$A_1 \oplus B_1 \oplus B_2$	$2A' \oplus A''$
T_{2u}	$E \oplus B_1$	$A' \oplus 2A''$	$E \oplus A_2$	$A_1 \oplus A_2 \oplus B_2$	$2A' \oplus A''$

face, the eigenstates of Q are classified according to the irreducible representations of that point group. Hence, c_n must become zero if u_{bulk} is attributed to a different irreducible representation from that of u_L^n .

In order to confront our estimation with the predictions of group theory, let us consider again the previous example of normal incidence along the (111) direction. In this case incident light has a $\mathbf{k}_{\parallel}=0$ component within the surface Brillouin zone associated with the {111} set of planes. Following the above-mentioned procedure, we employed a 32-monolayer bare opal slab to obtain the electric-field distribution in the space between the 16th and 17th layers, where the bulk configuration is assumed to be achieved. At the same time, the photonic dispersion relation of the infinite periodic system was also recalculated for increasing values of k_z . Figure 5 shows both the dispersion relation and symmetry assignment within the [1.10,1.3] interval. Now, we will pay particular attention to the pair of frequency values marked with horizontal lines: for one of them ($a/\lambda=1.15$) no uncoupled bands are predicted by group theory, while for the other ($a/\lambda=1.25$) some of those bands are expected. In the first case, we obtained $|c_n|^2$ equal to 0.689 and 0.348 for E bands with positive group velocity and $|c_n|^2=0.007,0.006$ for the ones with negative slope. When calculated for the higher frequency, the values of $|c_n|^2$ for $E(+)$ and $E(-)$ bands are {0.265, 0.377, 0.109, 0.035} and {0.085, 0.016, 0.098, 0.054}, respectively. With regards to the uncoupled bands (i.e., those with A_1 symmetry), their coefficients are less than 10^{-16} . Therefore we can conclude that light transmission is actually forbidden for such modes, as far as they do not contribute to the excited field inside the slab. This constitutes a confirmation of group-theory predictions.

VI. SUMMARY

We have analyzed the symmetry properties of eigenstates along the high-symmetry directions of close-packed bare opals according to the group theory. We found that some bands cannot be coupled with an external plane wave along several directions because of symmetry reasons, which was confirmed by layer-KKR calculations; nevertheless, the presence of uncoupled modes is not expected to provide any observable features in the transmittance for this particular system.

ACKNOWLEDGMENTS

The support of the European Commission, Project No. IST-1999-19009 PHOBOS, is gratefully acknowledged. We also acknowledge financial aid provided by the Spanish CICYT (Project No. MAT2000-1670-C04-04). F.L.T. and J.S.D. acknowledge the computing facilities provided by the Centro de Computación Científica at the universidad Autónoma de Madrid.

APPENDIX A: NUMERICAL ASSIGNMENT OF IRREDUCIBLE REPRESENTATIONS

As stated in Sec. III, the label assignment for a given mode $E_{\mathbf{k}}^n(\mathbf{r})$ is based on the evaluation of its character under

TABLE V. The compatibility relations of irreducible representations at the X point in the fcc lattice.

$X[D_{4h}]$	$\overline{\Gamma X}[C_{4v}]$	$\overline{XU}[C_{2v}]$	$\overline{XW}[C_{2v}]$
A_{1g}	A_1	A_1	A_1
A_{2g}	A_2	B_2	B_2
B_{1g}	B_1	B_2	A_1
B_{2g}	B_2	A_1	B_2
E_g	E	$A_2 \oplus B_1$	$A_2 \oplus B_1$
A_{1u}	A_2	A_2	A_2
A_{2u}	A_1	B_1	B_1
B_{1u}	B_2	B_1	A_2
B_{2u}	B_1	A_2	B_1
E_u	E	$A_1 \oplus B_2$	$A_1 \oplus B_2$

TABLE VI. The compatibility relations of irreducible representations at the L point in the fcc lattice.

$L[D_{3d}]$	$\overline{\Gamma L}[C_{3v}]$	$\overline{LW}[C_2]$	$\overline{LU}[C_{1h}]$	$\overline{LK}[C_{1h}]$
A_{1g}	A_1	A	A'	A'
A_{2g}	A_2	B	A''	A''
E_g	E	$A \oplus B$	$A' \oplus A''$	$A' \oplus A''$
A_{1u}	A_2	A	A''	A''
A_{2u}	A_1	B	A'	A'
E_u	E	$A \oplus B$	$A' \oplus A''$	$A' \oplus A''$

TABLE VII. The compatibility relations of irreducible representations at the U point in the fcc lattice.

$U[C_{2v}]$	$\overline{\Gamma U}[C_{1h}]$	$\overline{XU}[C_{2v}]$	$\overline{LU}[C_{1h}]$	$\overline{UW}[C_{1h}]$
A_1	A'	A_1	A'	A'
A_2	A''	A_2	A''	A''
B_1	A'	B_1	A'	A''
B_2	A''	B_2	A''	A'

TABLE VIII. The compatibility relations of irreducible representations at the W point in the fcc lattice.

$W[D_{2d}]$	$\overline{\Gamma W}[C_{1h}]$	$\overline{XW}[C_{2v}]$	$\overline{LW}[C_2]$	$\overline{UW}[C_{1h}]$	$\overline{WK}[C_{1h}]$
A_1	A'	A_1	A	A'	A'
A_2	A''	A_2	B	A''	A''
B_1	A''	A_2	A	A''	A''
B_2	A'	A_1	B	A'	A'
E	$A' \oplus A''$	$B_1 \oplus B_2$	$A \oplus B$	$A' \oplus A''$	$A' \oplus A''$

TABLE IX. The compatibility relations of irreducible representations at the K point in the fcc lattice.

$K[C_{2v}]$	$\overline{\Gamma K}[C_{2v}]$	$\overline{LK}[C_{1h}]$	$\overline{WK}[C_{1h}]$
A_1	A_1	A'	A'
A_2	A_2	A''	A''
B_1	B_1	A'	A''
B_2	B_2	A''	A'

the symmetry operators within $G_{\mathbf{k}}$. The first thing that needs to be remarked is that solutions obtained by means of the plane-wave expansion method (in fact by means of any numerical calculation) do not satisfy Eq. (17) except in an approximate way. However, a suitable algorithm can always be found in order to estimate the character of computed eigenfunctions.

In our present work, we have defined a strategy based on direct evaluation of Eq. (17), which will now be rewritten for the sake of clarity:

$$\mathbf{P}_g \equiv \hat{A} \mathbf{E}_g = \sum_{g'} \alpha_{g,g'} \mathbf{E}_{g'}. \quad (\text{A1})$$

In the case of one-dimensional irreducible representations ($g=1$), the character $\chi(\hat{A})$ is given by

$$\chi_{1D} = \alpha = \frac{\mathbf{P} \cdot \mathbf{E}}{|\mathbf{E}|^2}. \quad (\text{A2})$$

Similar expressions can be obtained for two-dimensional ($g \leq 2$) representations

$$\chi_{2D} = \sum_{j,k} \frac{(-1)^{j+k} [(\mathbf{P}_j \cdot \mathbf{E}_k)(\mathbf{E}_k \cdot \mathbf{E}_j) - (\mathbf{P}_j \cdot \mathbf{E}_j)|\mathbf{E}_k|^2]}{|\mathbf{E}_1|^2 |\mathbf{E}_2|^2 - (\mathbf{E}_1 \cdot \mathbf{E}_2)(\mathbf{E}_2 \cdot \mathbf{E}_1)}, \quad (\text{A3})$$

and also for three-dimensional ($g \leq 3$) ones, given that some auxiliary quantities be defined:

$$\chi_{3D} = \frac{\mathbf{w}_1 \cdot (\mathbf{v}_2 \times \mathbf{v}_3) + \mathbf{v}_1 \cdot (\mathbf{w}_2 \times \mathbf{v}_3) + \mathbf{v}_1 \cdot (\mathbf{v}_2 \times \mathbf{w}_3)}{\mathbf{v}_1 \cdot (\mathbf{v}_2 \times \mathbf{v}_3)}, \quad (\text{A4})$$

$$(\mathbf{v}_k)_j = \mathbf{E}_k \cdot \mathbf{E}_j, \quad (\text{A5})$$

$$(\mathbf{w}_k)_j = \mathbf{P}_k \cdot \mathbf{E}_j. \quad (\text{A6})$$

APPENDIX B: COMPATIBILITY RELATIONS OF IRREDUCIBLE REPRESENTATIONS IN THE FCC LATTICE

In Tables IV–IX, the compatibility relations between the irreducible representations for the points at the corners of the irreducible part of the fcc first Brillouin zone and those for the wave vectors on intermediate segments are presented. It can be observed that only one mirror reflection is defined on many of these segments because of their low-symmetry invariance.

*Author to whom correspondence should be addressed. Email address: fernando.lopeztejeira@uam.es

¹E. Yablonovitch, Phys. Rev. Lett. **58**, 2059 (1987).

²S. John, Phys. Rev. Lett. **58**, 2486 (1987).

³See, for instance, L. Martín-Moreno, F.J. García-Vidal, and A.M. Somoza, Phys. Rev. Lett. **83**, 73 (1999), and references therein; A more recent review can be found in Y. Xia, B. Gates, and Z.Y. Li, Adv. Mater. **13**, 409 (2001).

⁴R. Mayoral, J. Requena, S.J. Moya, C. López, A. Cintas, H. Míguez, F. Meseguer, L. Vázquez, M. Holgado, and A. Blanco, Adv. Mater. **9**, 257 (1997).

⁵Yu.A. Vlasov, V.N. Astratov, O.Z. Karimov, A.A. Kaplyanskii, V.N. Bogomolov, and A.V. Prokofiev, Phys. Rev. B **55**, 13 357 (1997).

⁶W. M. Robertson, G. Arjavalingam, R.D. Meade, K.D. Brommer, A.M. Rappe, and J.D. Joannopoulos, Phys. Rev. Lett. **68**, 2023 (1992).

⁷K. Sakoda, Phys. Rev. B **52**, 7982 (1995).

⁸T.F. Krauss, R.M. de la Rue, and S. Brand, Nature (London) **383**, 699 (1996).

⁹N. Stefanou, V. Karathanos, and A. Modinos, J. Phys.: Condens. Matter **4**, 7389 (1992).

¹⁰K. Ohtaka and Y. Tanabe, J. Phys. Soc. Jpn. **65**, 2670 (1996).

¹¹K. Sakoda, Phys. Rev. B **55**, 15 345 (1997).

¹²V. Karathanos, J. Mod. Opt. **45**, 1751 (1998).

¹³Z. Yuan, J.W. Haus, and K. Sakoda, Opt. Express **3**, 19 (1998).

¹⁴J.D. Joannopoulos, R.D. Meade, and J.N. Win, *Photonic Crystals* (Princeton University Press, Princeton, NJ, 1995).

¹⁵See, for instance, L.M. Falicov, *Group Theory and its Physical Applications* (University of Chicago Press, Chicago, 1966).

¹⁶A comprehensive investigation on the role of symmetry in photonic crystals can be found in K. Sakoda, *Optical Properties of Photonic Crystals* (Springer-Verlag, Berlin, 2001).

¹⁷J.E.G.J. Wijnhoven and W.L. Vos, Science **281**, 802 (1998).

¹⁸A.A. Zakhidov, R.H. Baughman, Z. Iqbal, C. Cui, I. Khayrullin, S.O. Dantas, J. Marti, and V.G. Ralchenko, Science **282**, 897 (1998).

¹⁹H. Míguez, F. Meseguer, C. López, M. Holgado, G. Andreasen, A. Mifsud, and V. Fornés, Langmuir **16**, 4405 (2000).

²⁰A. Blanco, E. Chomsky, S. Gratchak, M. Ibisate, S. John, S.W. Leonard, C. López, F. Meseguer, H. Míguez, J.P. Mondia, G. Ozin, O. Toader, and H.M. Van Driel, Nature (London) **405**, 437 (2000).

²¹H. Míguez, F. Meseguer, C. López, F. López-Tejeira, and J. Sánchez-Dehesa, Adv. Mater. **13**, 393 (2001).

²²S.G. Johnson and J.D. Joannopoulos, Opt. Express **8**, 173 (2001).

²³A. Reynolds, F. López-Tejeira, D. Cassagne, F.J. García-Vidal, C. Jouanin, and J. Sánchez-Dehesa, Phys. Rev. B **60**, 11 422 (1999).

²⁴N. Stefanou, V. Yannopoulos, and A. Modinos, Comput. Phys. Commun. **113**, 49 (1998); *ibid.* **132**, 189 (2000).

²⁵K. Ohtaka, Phys. Rev. B, **19**, 5057 (1979); J. Phys. C **13**, 667 (1980).

²⁶K. Ohtaka and Y. Tanabe, J. Phys. Soc. Jpn. **65**, 2276 (1996).

²⁷K. Ohtaka, T. Ueta, and K. Amemiya, Phys. Rev. B, **57**, 2550 (1998).

²⁸A. Modinos, N. Stefanou, and V. Yannopoulos, Opt. Express **8**, 197 (2001).

²⁹Further details can be found in T. Ochiai and J. Sánchez-Dehesa, Phys. Rev. B, **64**, 245113 (2001).